JOURNAL OF AIRCRAFT
Vol. 35, No. 6, November–December 1998

Comparison of Boundary-Layer Transition Predictions Using Flight Test Data

Géza Schrauf*
Daimler–Benz AG, Bremen D-28183, Germany
Jean Perraud†
ONERA, 31005 Toulouse Cedex 4, France
Domenico Vitiello‡
Alenia, 80038 Pomigliana d'Arco (NA), Italy
and
Fung Lam§
British Aerospace Airbus, Ltd., Bristol, England BS99 7AR, United Kingdom

Flight tests using a Fokker F100 aircraft equipped with a natural laminar flow glove demonstrated that natural laminar flow is feasible for transport aircraft with up to 130 passengers. Furthermore, the flight tests generated a wealth of experimental data. These data have been evaluated with all known variations of the e^N method. The aim of this investigation was to compare the different methods and to identify the one that yielded the best correlation. No clear winner turned up in our investigation; each method has its own merit. The envelope method, if based on a compressible stability theory with surface curvature effects, gives a valuable *N*-factor correlation. With this method, few pathological cases occurred. These were characterized by a measured transition behind the maximum of the computed *N* factors. Methods using the *N*-factor pairs (N_{TS}, N_β) and (N_{TS}, N_{CF}) computed with incompressible or compressible stability theory without curvature effects are also suitable. With these methods, however, many pathological cases occur. A satisfactory correlation can only be obtained if the pathological cases are excluded.

Introduction

LAMINAR flow on commercial aircraft is such a challenge that research programs are underway in the U.S. and Europe.[1] Expected reduction of friction drag should allow significant cost reductions, limiting fuel consumption and allowing some downsizing of structures. Within Europe, natural laminar flow (NLF) flight tests using a Fokker 100 aircraft were performed. The aircraft is a 130 seater, flying Mach 0.78, and allowing Reynolds numbers up to 3.4×10^7. Reasonable wing sweep was compatible with the use of a passive laminar flow glove installed on the wing to create a pressure distribution such that laminar–turbulent transition be delayed on both upper and lower wing surfaces.

The e^N method is the most sophisticated tool used in industry to predict laminar–turbulent transition. Because it is a correlation method, experimental results are needed for its calibration. In this paper, we give an overview of the evaluation of this experiment, using linear stability theory.

Most calculations have been done with the three codes, COAST, CASTET, and COSALX, an improved version of COSAL. These codes are based on the linear stability equations for compressible media including curvature. Additional calculations have been done with the incompressible codes COCIP and SALLY. References to these codes are given in Ref. 2.

Data Preparation

The glove was equipped with pressure taps along two sections parallel to the inner and outer edge. Transition was visualized on the upper and lower side of the glove using infrared thermography. Thus, for each flight measurement, four cases [I(nner)/O(uter section), L(ower)/U(pper side)] had to be considered. Selecting cases with clear infrared images and steady pressure data produced a set of 60 cases to be evaluated with linear stability theory. Measured pressure distributions were used for the three-dimensional boundary-layer calculation, prior to the stability analysis. Thorough validation of the calculation was done, which, however, cannot be presented here.

The first author performed an initial analysis of all 60 cases with incompressible stability theory. He divided the cases into three groups, A, B, and C, each containing all typical phenomena encountered, with the clearest cases in group A.

In the course of the evaluation, Schrauf[3] demonstrated that a new subset, M, namely the set with monotonically increasing envelopes, gives a comparatively better correlation for the methods with two *N* factors. The results presented in this paper are either for all cases, the A, or the M cases.

N-Factor Calculation

The e^N method for transition prediction is based on linear stability theory for disturbances described by a wave of the form

$$q'(x, y, z, t) = \hat{q}(z)\exp[i(\alpha x + \beta y - \omega t)] \qquad (1)$$

Herein, x and y are tangential coordinates, and z is the wall-normal coordinate. For spatial amplification, the (circumferential) frequency ω is real and the two wave numbers α and

Presented as Paper 97-2311 at the AIAA 15th Applied Aerodynamics Conference, Atlanta, GA, June 23–25, 1997; received Aug. 3, 1997; revision received April 6, 1998; accepted for publication July 5, 1998.

*Research Scientist, Department EFV. Member AIAA.
†Research Scientist, CERT, Department DMAE 2, Avenue Edouard Belin.
‡Research Scientist, Viale dell'Aeronautica; currently at Centro Italiano Ricerche Aerospaziali, via Maiorise, 81043 Capua (CE), Italy.
§Research Scientist, B61 Wing Aerodynamics, P.O. Box 77, 7DO.

β are complex. Their real as well as imaginary parts can be written as follows:
Wave number (the wavelength λ is $2\pi/\sqrt{\alpha_r^2 + \beta_r^2}$)

$$\sqrt{\alpha_r^2 + \beta_r^2}$$

Propagation direction [the angle between the α direction, i.e., in this paper, the direction of the flow at the edge of the boundary layer, and the propagation direction is computed as $\varsigma = \arctan(\beta_r/\alpha_r)$]

$$1/\sqrt{\alpha_r^2 + \beta_r^2}\begin{pmatrix}\alpha_r\\ \beta_r\end{pmatrix}$$

Spatial amplification rate

$$\pm\sqrt{\alpha_i^2 + \beta_i^2}$$

Amplification direction

$$1/\sqrt{\alpha_i^2 + \beta_i^2}\begin{pmatrix}\alpha_i\\ \beta_i\end{pmatrix}$$

Using the ansatz (1), we obtain the Orr–Sommerfeld equation for incompressible media and a system of ordinary differential equations for compressible media. This constitutes sufficient information to compute the complex wave number α for a given frequency ω in two-dimensional flows in which propagation direction and amplification direction coincide with the direction of the flow.

In three-dimensional flows, a second complex wave number β appears, and we must find two additional conditions to close the problem.

Rigorous extension to three dimensionality can only be done in the case of an infinitely long, swept wing. In this case, the spanwise wave number component of each instability wave remains constant. Furthermore, the amplification direction, i.e., the direction in which we observe the wave amplification, can be chosen arbitrarily because all flow quantities are independent of the spanwise position. As an amplification direction we can choose the direction perpendicular to the leading edge, the direction of the streamline at the boundary-layer edge, or the direction of the group velocity. Using the two latter directions, we observe less amplification. However, the length of the integration path becomes larger so that the same N factor is obtained.

Thus, for an infinitely long, swept wing, the two additional conditions are the spanwise wave number condition and the choice of the amplification direction. The N factor computed under those conditions is called N_β.

In the general case, the amplification direction can not be chosen arbitrarily. Because the direction of the group velocity is the direction of energy transport for propagating waves, we choose this direction as the amplification direction. (If the numerical method solves the temporal problem, the group velocity direction is used by Mack's extension of the Gaster transformation to three dimensions.) This constitutes the first additional condition.

To motivate a possible second condition, we consider the stripe pattern observed in the visualization of crossflow-dominated transition. The stripes have an approximately constant width. They are caused by stationary crossflow waves, the wavelength of which corresponds to the width within the pattern. Based on this observation, we consider instability waves with a constant frequency and, additionally, with constant wavelength. If we integrate their local amplification rates, we obtain the N_λ factor. If the frequency is chosen to be 0 Hz, i.e., if we consider only stationary crossflow waves, the N_λ factor is written as N_{CF}.

Another N factor is obtained by tracing waves with constant propagation direction $\varsigma = \arctan(\beta_r/\alpha_r)$. This N factor is denoted by N_ς. If the propagation direction is chosen to be the direction of the inviscid flow at the boundary-layer edge, i.e., if $\varsigma = 0$ deg, it is called N_{TS}.

The propagation directions of the instability waves that cause transition are not known a priori. One can compute the ς envelope of the N_ς factor curves for each direction ς and afterward form the envelope of all N_ς envelopes. This method is called the "envelope-of-envelopes" method. It is different from the classical envelope method that uses the wave with maximal amplification at each position of the boundary layer. To our knowledge, the F100 flight tests are the first ones systematically evaluated with this method.[2]

Envelope Method

For each N-factor strategy, the analysis of the flight experiment was started with a thorough validation of the calculated stability results. As an example, Fig. 1 shows the local propagation directions obtained with the envelope method by different partners for a case with $M_\infty = 0.7$, $Re = 21.7 \times 10^6$, $\varsigma_{LE} = 19.7$ deg (case 319OU).

We observe the typical behavior encountered for swept wings, namely that crossflow (CF) amplification is dominant in the neighborhood of the leading edge, and that Tollmien–Schlichting (TS) amplification becomes dominant farther downstream. Using the envelope, we look at each boundary-layer station for the wave with the largest amplification rate, and find a jump from crossflow to TS amplification. The jump is not visible in the local amplification rates, because it occurs when both rates have nearly the same magnitude (cf. Fig. 2). It can take place earlier or later, depending on the settings used in the codes.

A complete analysis for this case, using the envelope method with compressible stability theory including curvature effects, is presented in Fig. 3. For this case, transition was observed between 16 and 18% chord. The correlation with the middle of the transition region is indicated by the arrows.

The N factors of all group A cases obtained with the envelope method using the compressible stability theory with curvature effects are shown in Fig. 4. The ONERA/CERT results, for example, vary from $N = 8.75$ to 16.2 with an average of $N = 12.6$. A comparison with incompressible stability theory is shown in Fig. 5.

The results for group M, obtained with the envelope method, are shown in Fig. 6. In contrast to the methods with two N

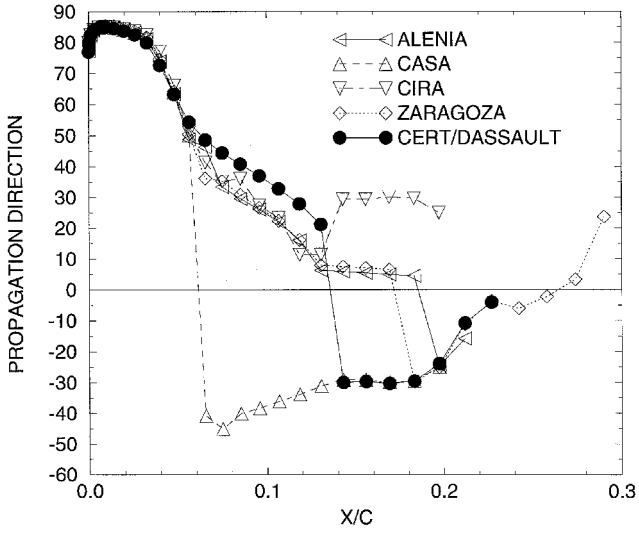

Fig. 1 Local wave propagation direction computed with the envelope method using compressible stability theory with curvature effects.

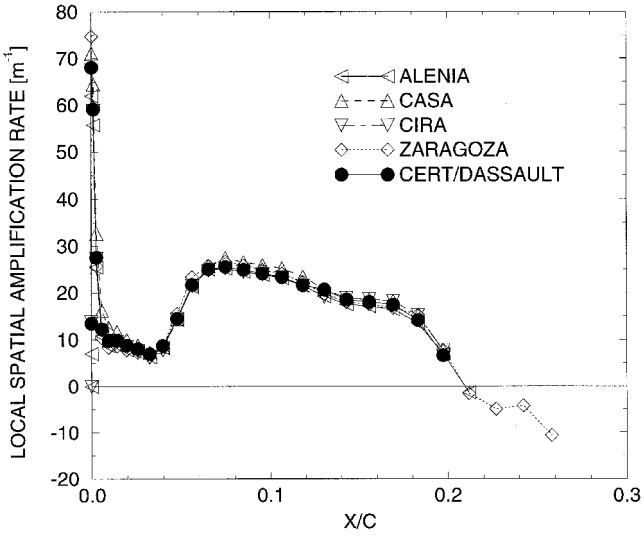

Fig. 2 Local spatial amplification rates computed with the envelope method using compressible stability theory with curvature effects.

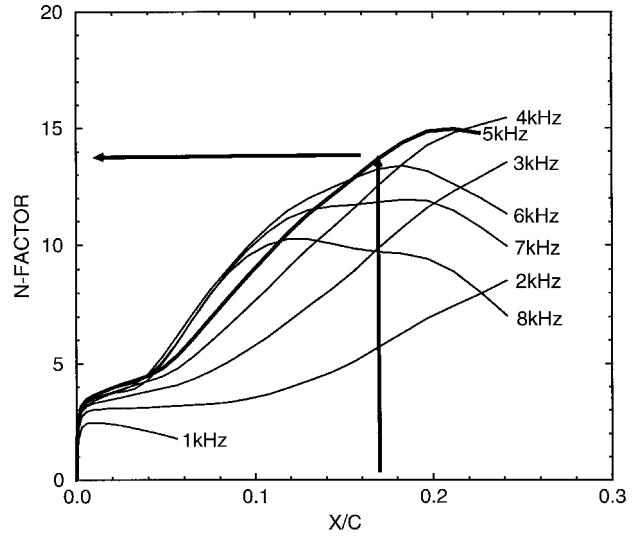

Fig. 3 Envelope *N* factors for different frequencies computed with compressible stability theory with curvature.

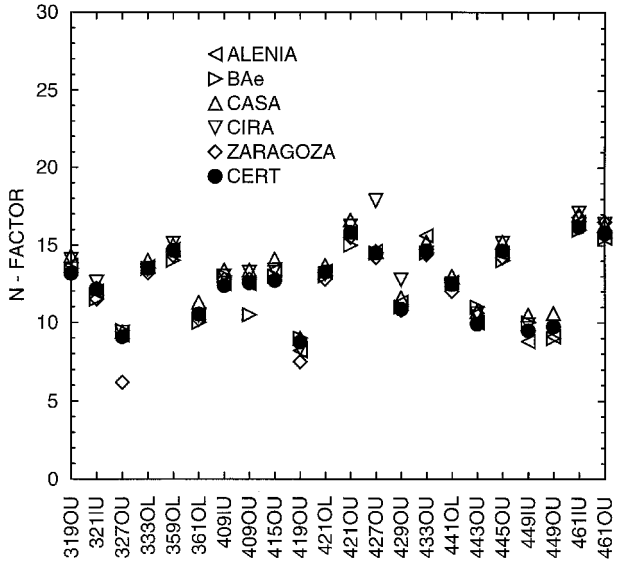

Fig. 4 *N* factors of group A obtained with the envelope method using compressible stability theory with curvature.

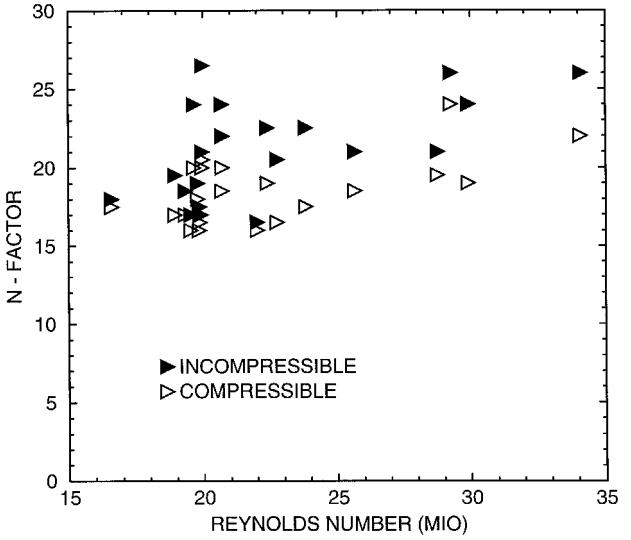

Fig. 5 *N* factors of the new subgroup obtained with the envelope method using compressible as well as incompressible stability theory without curvature.

factors, there is no improvement in *N*-factor correlation. The *N* factors vary from $N = 9.75$ to 19.7, with an average of 13.8 for compressible stability theory with curvature effects and without curvature effects, from 17 to 25.2 with an average of 20.6.

To improve our analysis, we searched for characteristic properties that would allow us to classify the measurements into groups. The correlation should then give a typical *N* factor with less scatter for each group. In Fig. 7, the correlated *N* factors of group M vs the propagation direction of the wave that contributes to the envelope curve at transition was plotted. We obtain no results with propagation directions between 46 and 73 deg. This allowed us to distinguish between CF- and TS-dominated transitions. CF-dominated transitions are cases with propagation direction above 70 deg and TS-dominated transitions are those with the propagation direction up to around 45 deg.

Using the approach with two *N* factors, we also find those two categories. There is no ambiguity, i.e., there is no case that would be called CF dominated based on the envelope method and TS dominated if an approach with two *N* factors is used.

In Fig. 8, we plot the results over the Reynolds number. Here, the *N* factors of the CF-dominated cases lie nearly on one level, whereas the *N* factors of the TS-dominated cases exhibit considerable scatter. To reduce the scatter, we subdivide the TS-dominated cases into two groups. (Such a classification is less obvious and can only be done if we consider the results of the envelope method together with the results of the approach with two *N* factors.)

1) *Clear TS-dominated cases*: These are cases for which the crossflow *N* factor $N_{CF,i}$, obtained with incompressible stability theory, stays well below the limit of nine; or if this limit is exceeded, it is done only briefly and crossflow is strongly damped at transition.

2) *TS-dominated cases with strong crossflow amplification*: These are TS-dominated cases for which the crossflow *N* factor $N_{CF,i}$ obtained with incompressible stability theory exceeds the value of nine and stays at a higher level.

In Fig. 9, the different categories are plotted vs Reynolds numbers. For each category we include the linear regression line that minimizes the quadratic error. We obtain a horizontal line for the crossflow cases, i.e., the *N* factor is indeed independent of the Reynolds number (universal). The regression

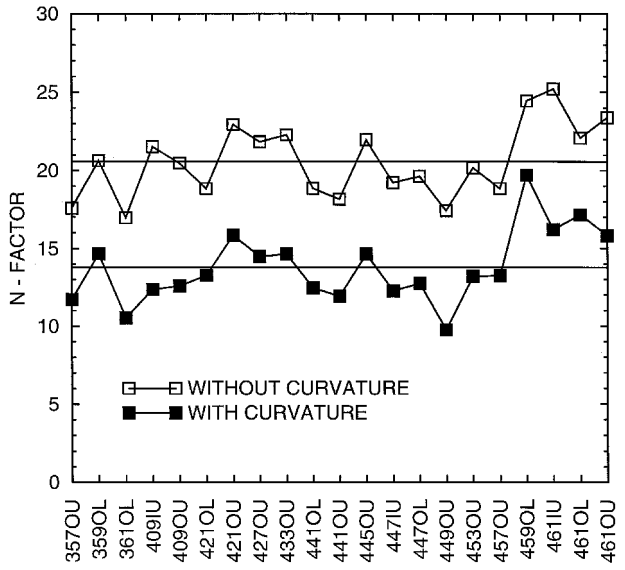

Fig. 6 *N* **factors of the new subgroup obtained with the envelope method using compressible stability theory.**

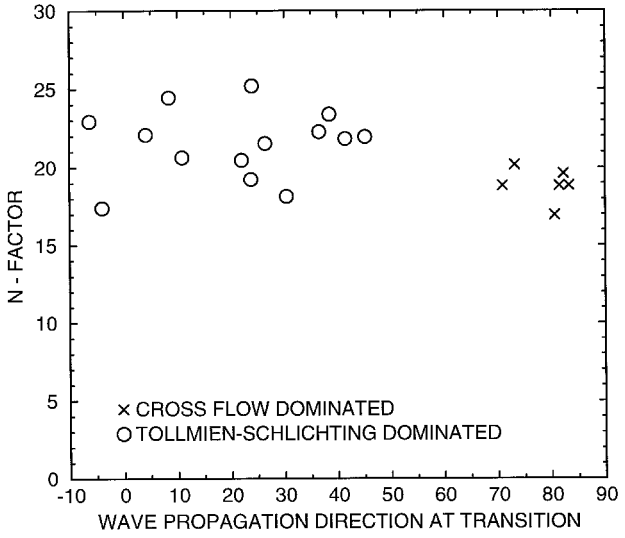

Fig. 7 *N* **factors vs propagation direction of the wave contributing to the envelope curve at transition.**

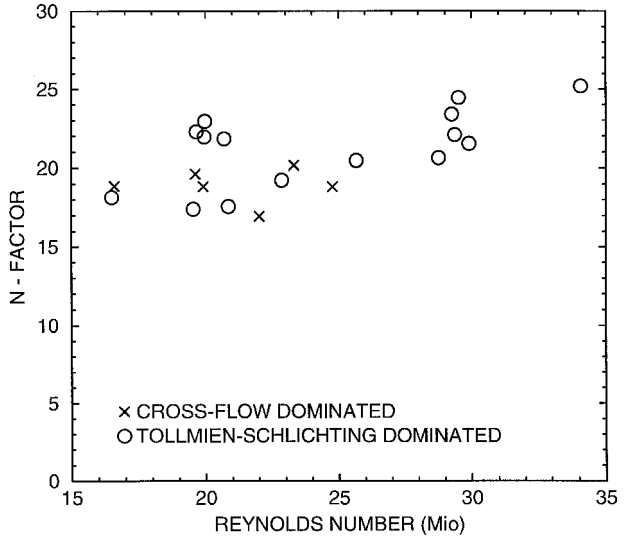

Fig. 8 *N* **factors vs Reynolds number.**

lines for each of the two TS-dominated cases increases monotonically, i.e., the correlated *N* factor depends on the Reynolds number. The scatter, however, becomes much smaller. The *N* factors of the clear TS-dominated cases are smaller than the ones with strong CF amplification. In those cases, the strong CF amplification near the leading edge lifts the *N* factor to a higher level before the TS amplification can contribute to the *N* factor. The same phenomenon was observed in the ATTAS flight experiments.[4]

The results in Fig. 9 are obtained by using linear stability theory without curvature effects. If surface curvature is taken into account, we obtain the qualitatively similar results shown in Fig. 10. The inclusion of surface curvature effects reduces the calculated amplification rates (cf. Ref. 5), and we obtain smaller *N* factors. Because the reduction mainly affects the CF waves, the difference between the pure TS cases and the TS cases with strong CF amplification becomes smaller. Without curvature effects, *N* factors from 17.0 to 25.2 with a mean value of 20.7 are obtained for the pure TS cases. Taking surface curvature effects into account, the mean value becomes 13.8 with a variation from 9.7 to 19.7. In conclusion, no universal *N* factor has been obtained with the envelope method. However, only two pathological cases occurred, i.e., cases for which transition occurs behind the maximal *N* factor.

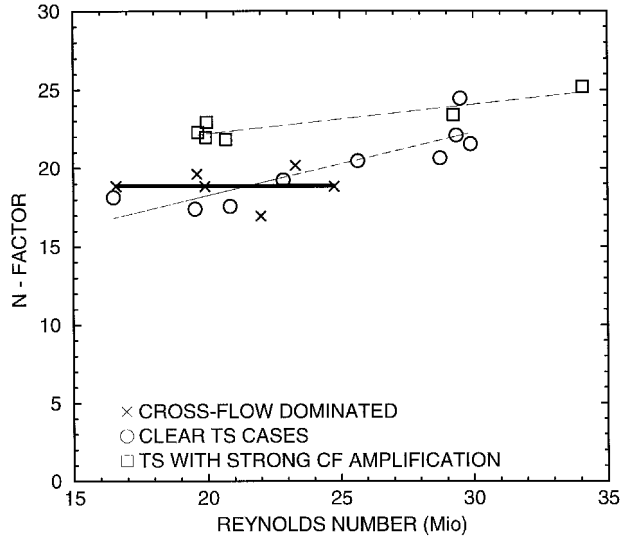

Fig. 9 *N* **factors computed with compressible stability theory without curvature effects.**

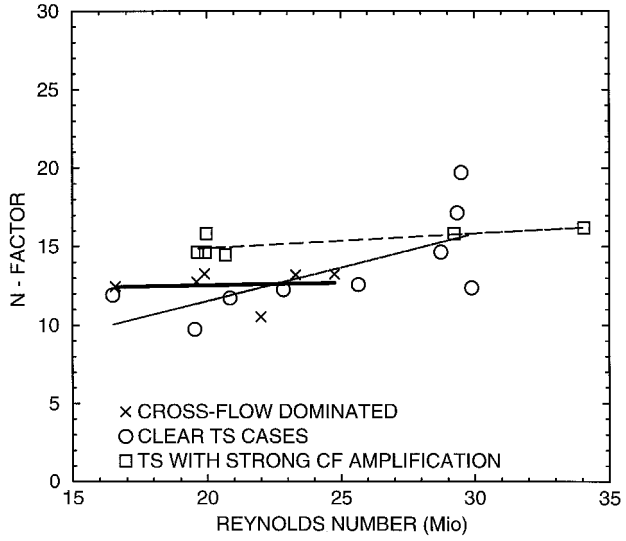

Fig. 10 *N* **factors computed with compressible stability theory with curvature effects.**

Methods Based on Two *N* Factors

We now consider transition prediction methods based on two different *N* factors, one for TS waves and a second one for CF flow waves. The first *N* factor is the N_{TS} factor of the prescribed frequency/prescribed propagation direction strategy. It is shown that the difference between the 0 deg-direction and the direction yielding the largest N_s is small for swept wings of transport aircraft flying at transonic speeds.[2] Therefore, we can restrict the computations to 0-deg waves.

For the second *N* factor describing the amplification of crossflow waves, we consider two choices: an *N* factor computed with the prescribed frequency/prescribed wavelength strategy, and the *N* factor computed with the prescribed frequency/prescribed spanwise wave number strategy for an infinitely long, swept wing. Experiments show that stationary crossflow waves dominate the transition process in a low-turbulence environment, whereas traveling crossflow waves dominate the transition in a high-turbulence environment.[6,7] Therefore, we consider only stationary crossflow waves, as we assume that stationary crossflow waves play the most important role inducing transition on a swept wing.

In Fig. 11, we show the *N* factors of stationary crossflow waves for several wavelengths obtained with incompressible stability theory without curvature effects for a case with stronger crossflow amplification [$M_\infty = 0.78$, $Re = 21.7\ 10^6$, $s_{LE} = 22.4a$, (case 427OU)].

We see that short waves predominate in the neighborhood of the leading edge whereas longer waves predominate farther downstream. This behavior reflects the very rapid thickening of the boundary layer close to the leading edge. Figure 12 shows the spanwise wave number of the stationary crossflow wave with wavelength $0.0045m$. The spanwise wave number changes largely near the leading edge, where the flow turns from the spanwise to the chordwise direction. Farther downstream, the changes in flow direction are smaller. There, a wave with a constant wavelength exhibits only a small varia-

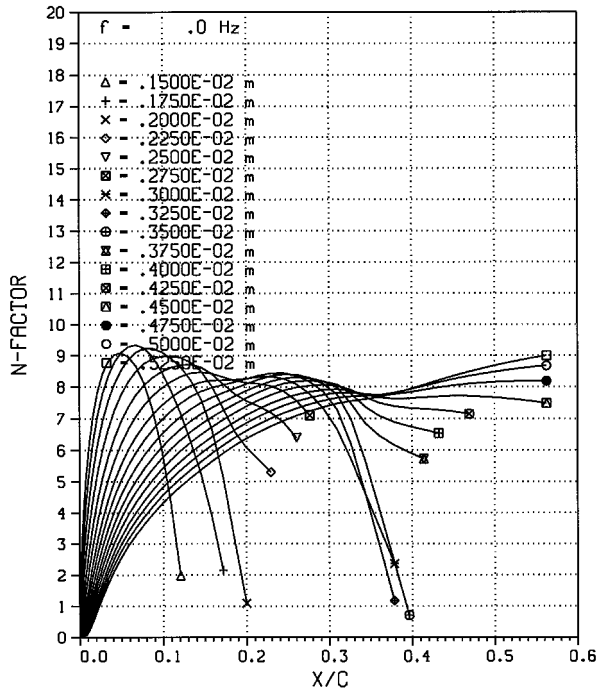

Fig. 11 N_{CF} **factors computed with incompressible stability theory for measurement 427OU.**

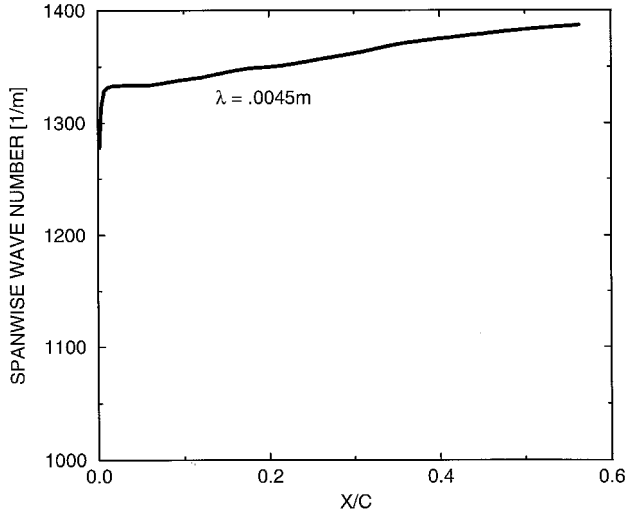

Fig. 12 Spanwise wave number of the $\lambda = 0.0045m$ **wave in Fig. 11.**

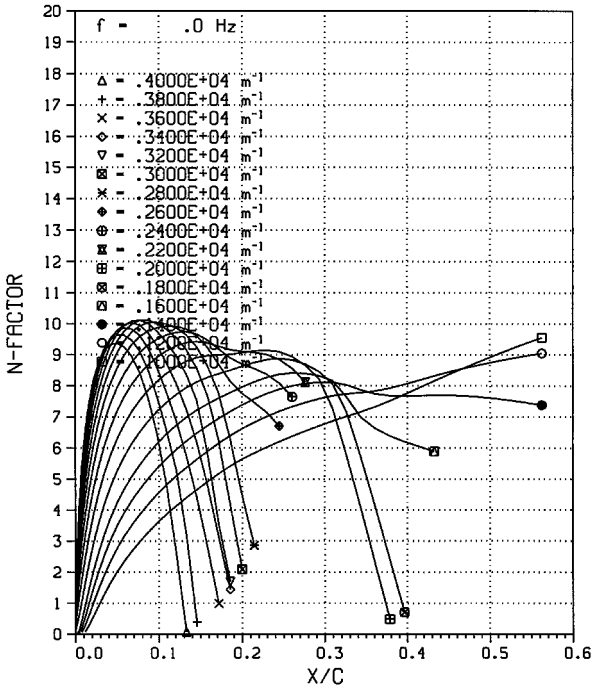

Fig. 13 N_β **factors computed with incompressible stability theory for measurement 427OU.**

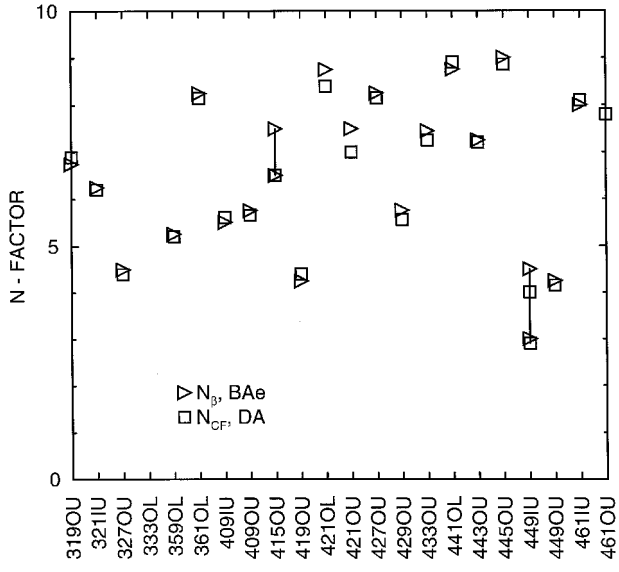

Fig. 14 Comparison of N_β **and** N_{CF}.

tion in the spanwise wave number. As waves with a relatively long wavelength (or small wave number) are mainly amplified in that downstream region, the correlated N_{CF} and N_{β} factors are comparable (cf. Figs. 11 and 13) if transition does not occur too close to the leading edge. This should be the case for laminar wings.

A comparison of the correlated N_{CF} and N_{β} factors is shown in Fig. 14. We see that, for the F100 glove, both *N*-factor integration strategies are equivalent.

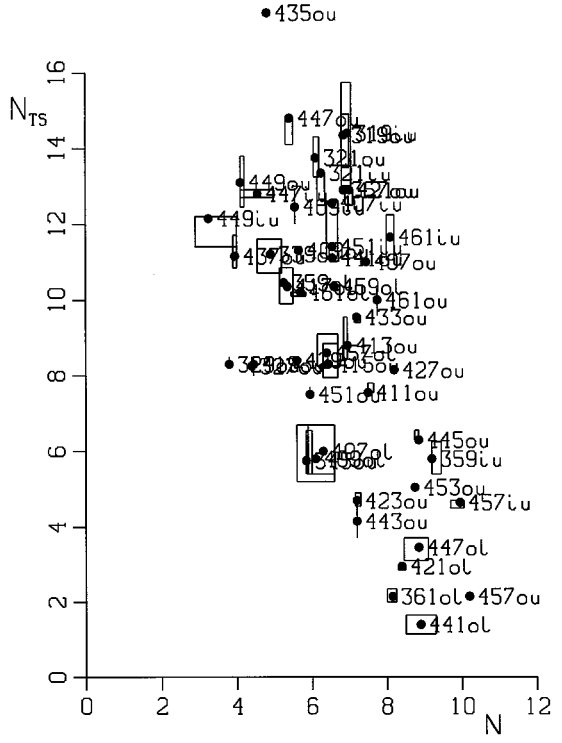

Fig. 15 Correlated (N_{CF}, N_{TS}) pairs obtained with incompressible stability theory for all measurements.

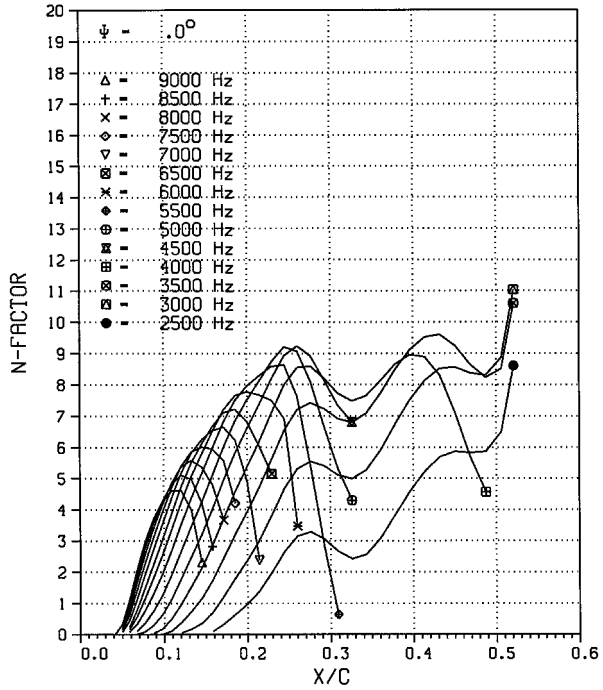

Fig. 16 N_{TS} factors computed with incompressible stability theory for measurement 451OU.

Having described the two possible choices of the second *N* factor, we present the pairs of correlated (N_{CF}, N_{TS}) factors obtained with incompressible stability theory without curvature effects in Fig. 15. The pairs form a cloud with no clear border at the inner edge. This situation is not improved by applying compressible stability theory.

This unsatisfactory correlation is a result of cases such as the one shown in Figs. 16 and 17 [$M_{\infty} = 0.7$, $Re = 22 \times 10^6$, $s_{LE} = 19.8$ deg, (case 451OU)], for which transition occurs at 31–34%, i.e., behind a local maximum of the envelope curve.

In those cases, transition cannot be predicted by classical stability theory. To continue using the F100 flight tests for *N*-factor correlation, Schrauf[3] proposed considering cases with monotonically increasing *N* factor envelopes only. For those cases, nonlocal and/or nonlinear effects, as, for example, sat-

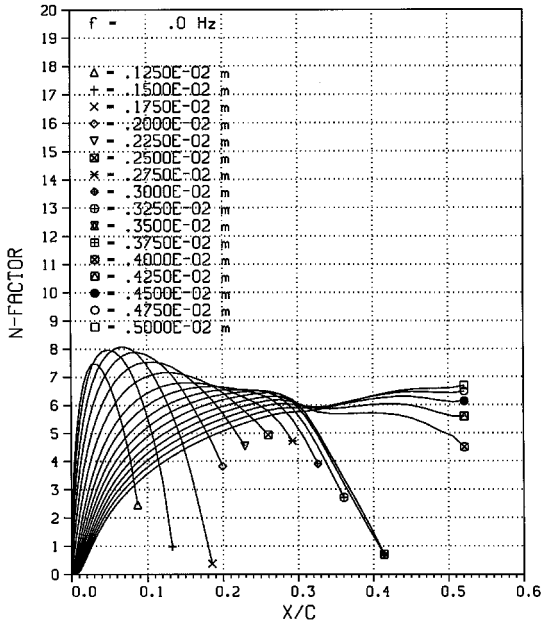

Fig. 17 N_{CF} factors computed with incompressible stability theory for measurement 451OU.

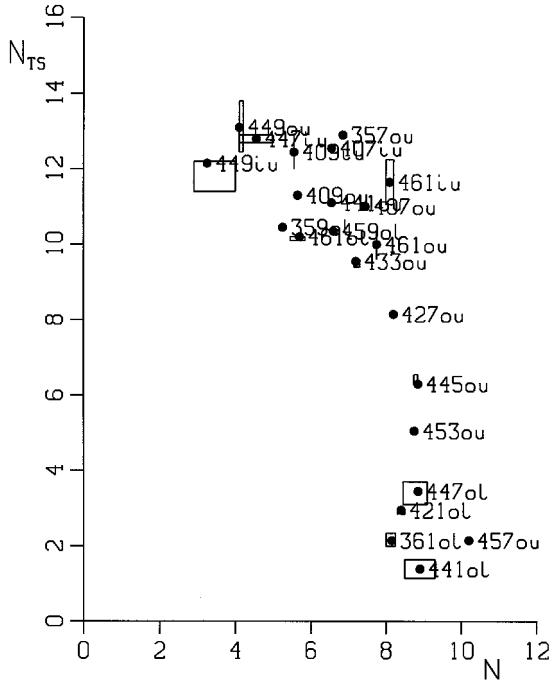

Fig. 18 Correlated (N_{CF}, N_{TS}) pairs obtained with incompressible stability theory for the new subgroup of monotonic cases.

uration effects observed for crossflow-dominated transition in another flight test,[8] are obviously surpassed by continuing linear amplification, so that linear amplification, described by classical theory, dominates transition.

The (N_{CF}, N_{TS}) pairs of these cases, obtained with incompressible stability theory, are shown in Figure 18. They exhibit a much clearer inner edge so that these results can be used for transition prediction with the e^N method.

Conclusions

Four different N-factor integration strategies have been considered. The envelope method and strategies prescribing the frequency and, as a second condition, the spanwise wave number, the wavelength, or the propagation direction of the instability wave. The strategies can be grouped into two different N-factor methods for transition prediction. No method is clearly superior, each method has its merits and drawbacks.

1) *Envelope method*: If based on a compressible stability theory with surface curvature effects, we obtain a valuable N-factor correlation that can be used by the design engineer. The correlation can be improved if we distinguish between crossflow-dominated, TS-dominated, and mixed cases. In only 2 out of 32 cases the envelope method transition did occur behind the N factor maximum. These cases were labelled "pathological."

2) *Methods based on two N-factors*: For typical swept, transonic wings of transport aircraft, the methods based on (N_{TS}, N_{β}) and (N_{TS}, N_{CF}) factors are equivalent. Incompressible or compressible stability theory without curvature effects should be used. A good correlation is obtained for monotonically increasing cases. However, half of the 60 flight measurements are pathological, i.e., transition occurs behind an N-factor maximum.

Despite its limitations, the e^N method is the best tool available for transition prediction. In the hands of an experienced design engineer, who is aware of its peculiarities, the e^N method can be a very useful tool for natural laminar flow and hybrid laminar flow wing design.

Acknowledgments

The Fokker 100 flight tests were performed within the ELFIN program and the evaluation within the ELFIN II program. Both programs were sponsored by the European Commission. D. Vitiello's contribution to this paper was given during tenure as Alenia representative to the ELFIN project. We thank H. W. Stock, Dornier; A. Abbas, CASA; J. P. Tribot, Dassault; Y. Sedin, SAAB; D. Arnal, ONERA/CERT; R. S. Donelli and P. de Matteis, CIRA; W. Schröder, DLR Braunschweig; D. Rozendal, NLR; J. M. M. Sousa, I.S.T Lisboa; and I. Garrido and A. Pascau, University of Zaragoza, for their contributions to the work of ELFIN II Task 2.

References

[1]Arnal, D., and Bulgubure C., "Drag Reduction by Boundary Layer Laminarization," *La Recherche Aérospatiale*, Vol. 3, 1996, pp. 157–165.

[2]Schrauf, G., Perraud, J., Vitiello, D., Lam, F., Stock, H. W., and Abbas, A., "Transition Prediction with Linear Stability Theory—Lessons Learned from the ELFIN F100 Flight Demonstrator," *Proceedings of 2nd European Forum on Laminar Flow Technology*, AAAF, Paris, France, 1996, pp. 58–71.

[3]Schrauf, G., "Stability Analysis of the F100 Flight Experiment–A Second Look," ELFIN II TR 173, Jan. 1996.

[4]Schrauf, G., "Transition Prediction Using Different Linear Stability Analysis Strategies," AIAA Paper 94-1848, June 1994.

[5]Schrauf, G., "Curvature Effects for Three-Dimensional Compressible Boundary-Layer Stability," *Zeitschrift für Flugwissenschaften und Weltraumforschung*, Vol. 16, No. 2, 1992, pp. 119–127.

[6]Bippes, H., "Instability Features Appearing on Swept Wing Configurations," *Laminar-Turbulent Transition*, edited by D. Arnal and R. Michel, Springer–Verlag, Berlin, 1990.

[7]Deyhle, H., and Bippes, H., "Disturbance Growth in an Unstable Three-Dimensional Boundary Layer and Its Dependence on Environmental Conditions," *Journal of Fluid Mechanics*, Vol. 316, 1996, pp. 73–113.

[8]Herbert, T., and Schrauf, G., "Crossflow-Dominated Transition in Flight Tests," AIAA Paper 96-0185, Jan. 1996.